Open Access



RESEARCH ARTICLE

### Investigating boreal forest successional stages in Alaska and Northwest Canada using UAV-LiDAR and RGB and a community detection network

Léa Enguehard<sup>1</sup> (i), Birgit Heim<sup>1</sup>, Ulrike Herzschuh<sup>1,2,3</sup>, Viktor Dinkel<sup>1</sup>, Glenn Juday<sup>4</sup>, Santosh Panda<sup>5</sup>, Nicola Falco<sup>6</sup>, Jacob Schladebach<sup>1</sup>, Jakob Broers<sup>1</sup> & Stefan Kruse<sup>1</sup>

#### Keywords

LiDAR, Network, North American Boreal Forest, Successional Stage, UAV

#### Correspondence

Léa Enguehard and Stefan Kruse, Polar Terrestrial Environmental Systems, Alfred Wegener Institute Helmholtz Centre for Polar and Marine Research, Potsdam, Germany. Email: lea.enguehard@awi.de and stefan. kruse@awi.de

Editor: Dr. Temuulen Sankey Associate Editor: Dr. Wang Li

Received: 12 March 2025; Revised: 18 June 2025; Accepted: 28 July 2025

doi: 10.1002/rse2.70029

### **Abstract**

Boreal forests are a key component of the global carbon cycle, forming North America's most extensive biome. Different successional stages in boreal forests have varying levels of ecological values and biodiversity, which in turn affect their functions. A knowledge gap remains concerning the present successional stages, their geographic patterns and possible successions. This study develops a novel application of UAV-LiDAR and Red Green Blue (RGB) data and network analysis to enhance our understanding of boreal forest succession. Between 2022 and 2024, we collected UAV-LiDAR and RGB data from 48 forested sites in Alaska and Northwest Canada to (i) identify present successional stages and (ii) deepen our understanding of successional trajectories. We first applied UAV-derived spectral and structural tree attributes to classify individual trees into plant functional types representative of boreal forest succession, amely, evergreen and deciduous. Second, we built a forest-patch network to characterize successional stages and their interactions and assessed future stage transitions. Finally, we applied a simplified forward model to predict future dynamics and highlight different successional trajectories. Our results indicate that tree height and spectral variables are the most influential predictors of plant functional type in random forest algorithms, and high overall accuracies were attained. The network-based community detection algorithm reveals five interconnected successional stages that could be interpreted as ranging from early to late successional and a disturbed stage. We find that disturbed sites are mainly located in Interior and Southcentral Alaska, while late successional sites are predominant in the southern Canadian sites. Transitional stages are mainly located near the tundra-taiga boundary. These findings highlight the critical role of disturbances, such as fire or insect outbreaks, in shaping forest succession in Alaska and Northwest Canada.

### Introduction

Boreal forests are a critical component of the global carbon cycle and are valued globally for their ecological services (Bonan et al., 1992; Gauthier et al., 2015; Pan et al., 2011). They form North America's most extensive

biome, covering 30% of its surface north of Mexico and spanning a vast transcontinental crescent (Barbour & Christensen, 1993; Weber & Van Cleve, 2005). In Alaska and Northwest Canada, boreal forests are characterized by low tree species biodiversity, largely dominated by coniferous species mixed with broadleaf deciduous trees (Kayes

<sup>&</sup>lt;sup>1</sup>Polar Terrestrial Environmental Systems, Alfred Wegener Institute Helmholtz Centre for Polar and Marine Research, Potsdam, Germany

<sup>&</sup>lt;sup>2</sup>Institute for Environmental Science and Geography, University of Potsdam, Potsdam, Germany

<sup>&</sup>lt;sup>3</sup>Institute for Biochemistry and Biology, University of Potsdam, Potsdam, Germany

<sup>&</sup>lt;sup>4</sup>College of Natural Science and Mathematics, University of Alaska Fairbanks, Fairbanks, Alaska, USA

<sup>&</sup>lt;sup>5</sup>Institute of Agriculture, Natural Resources and Extension, University of Alaska Fairbanks, Fairbanks, Alaska, USA

<sup>&</sup>lt;sup>6</sup>Earth and Environmental Sciences, Lawrence Berkeley National Laboratory, Berkeley, California, USA

& Mallik, 2020; Van Cleve et al., 1991), with their composition changing over time through forest succession. Knowledge of the state and dynamics of forest succession is essential for effectively managing boreal forests amid global change (Kuuluvainen & Gauthier, 2018).

Forest succession is the gradual or abrupt change in the composition of ecological communities following a disturbance, most often fire or insect outbreaks in the Arctic region (Grime, 1979). This process unfolds through several phases, known as secondary successional stages (Grime, 1979; Huston & Smith, 1987). In Alaska and Northwest Canada, deciduous communities typically dominate earlier, while evergreen communities dominate late successional stages (Fastie & Ott, 2006; Massey et al., 2023; Ustin & Xiao, 2001). Old-growth forests have significantly higher ecological value and biodiversity than early successional stages (Bergeron & Fenton, 2012; Kuuluvainen, 2009), offering diverse habitats and essential ecosystem services, including long-term atmospheric carbon sequestration (Lafleur et al., 2018; Vedrova et al., 2018) and regulation of regional and local weather regimes (Watson et al., 2018). Several studies investigate the successional trajectories of forests in Alaska and Canada (Anyomi et al., 2022), yet a knowledge gap remains in understanding which successional stages are present, their geographic distribution and possible trajectories. While succession is traditionally studied through site-specific forest inventories, these methods can be limited in capturing larger-scale patterns. Advances in structural data gathered from Unmanned Aerial Vehicles (UAVs) offer a novel approach to analyzing these dynamics.

Stand structure is a fundamental attribute of forest ecosystems, reflecting their development, habitat suitability and shaping ecological functions (Bergen et al., 2009; Shugart et al., 2010; Worsham et al., 2025). Over the past decade, airborne LiDAR (Light Detection And Ranging) has become a key technology for capturing structural information at the landscape scale and is increasingly used coupled with field forest inventories (White et al., 2016). UAVs offer a cost- and time-effective solution for acquiring high-resolution imagery, making them particularly valuable for surveying remote boreal forest areas (Guimarães et al., 2020). As a result, UAV point cloud data are increasingly used in forestry for applications such as forest characterization (Alonzo et al., 2018; Brede et al., 2021), biomass estimation (Lu et al., 2020; Maesano et al., 2022), and conservation efforts (Belmonte et al., 2020; Scheeres et al., 2023), but have yet to be used to investigate boreal forest successional trajectories.

Several studies have demonstrated the effectiveness of LiDAR-derived metrics in characterizing structurally diverse mixed-species forests (Falkowski et al., 2009) and differentiating distinct successional stages in a mixed mature forest (Van Ewijk et al., 2011). More recently, UAV-borne LiDAR has been utilized to detect successional stage changes through canopy structural attributes (Almeida et al., 2020) and to distinguish forest types (Scheeres et al., 2023), though these applications focused on tropical landscapes. Despite these advancements, the potential for UAV-LiDAR and Red Green Blue (RGB) data to identify boreal forest successional stages remains largely unexplored. One approach to addressing this gap is network analysis, which provides a framework for examining connections between successional stages.

In ecological studies, network analysis models and seeks to understand the connections and interactions (i.e. edges) between individual elements (i.e. nodes) within an ecological system (Lau et al., 2017). In forest ecosystems, a network can be constructed to represent the relationships between successional stages, where the edges show the direction from one node to another by some process like succession. For example, Aquilué et al. (2020) evaluated the ecological resilience of forest patches for alternative management strategies based on network properties such as connectivity. Fuller et al. (2008) used network analysis to characterize tropical forest structure. Further, Zhang et al. (2023) explored the connection between forest patches and carbon stock distribution using a forest ecospatial network. Community detection algorithms applied to such networks enable the identification of clusters of forest patches with similar characteristics and provide insights into how different patches are related (Fortunato & Newman, 2022). While traditional clustering methods identify groups of similar forest patches, network analysis enables examination of the structure and dynamics of transitions between stages, offering insights into connectivity, succession pathways and system resilience that clustering approaches cannot capture. Yet despite its strengths, network analysis has not been used to identify successional stages based on structural remote sensing data.

This study leverages UAV-LiDAR coupled with RGB data and network analyses to (i) identify present successional stages in boreal forests and (ii) deepen our understanding of successional trajectories. Spanning 48 mapped areas across Alaska and Northwest Canada, this study covers a wide range of boreal forest landscapes where fieldwork was conducted between 2022 and 2024. We aim to answer the following questions: How are the forest patches we covered organized in a community network, and can we identify ecologically meaningful communities that represent successional stages and their potential trajectories? Specifically, we seek to determine which stages are present at the sites and if we can predict their development over time. First, we used UAV-based LiDAR to

.onlinelibrary.wiley.com/doi/10.1002/rse2.70029 by Helmh

Potsdam GFZ, Wiley Online Library on [10/11/2025]. See the Term:

segment and classify individual trees into plant functional types. Next, we built a forest-patch network to identify successional stages and their interactions. Finally, we mapped the identified stages and assessed future stage transitions. We hypothesize that UAV-LiDAR-derived metrics are essential for accurately classifying plant functional types (PFTs) and that network analysis can effectively identify distinct forest successional stages.

### **Materials and Methods**

### Study area and data acquisition

This study focuses on boreal forests in Northwest America, specifically Alaska and Northwest Canada. In the summers of 2022 to 2024, we collected data to explore boreal forest structure across 48 sites located between latitudes 60° N and 68.5° N and longitudes 127.5° W and 163.5° W (Fig. 1). This area spans from arctic treelines to dense forests in the subarctic south and portrays a mosaic of forest stands dominated by white spruce (*Picea glauca*), black spruce (*Picea mariana*), birch (*Betula neoalaskana*), aspen (*Populus tremuloides*) and poplar (*Populus balsamifera*). It covers a wide range of ecoregions, such as the Interior Alaska-Yukon lowland and alpine taiga and tundra regions in Alaska and Canada and the Northwest Territories taiga transgressing

northward to the treeline into the Canadian Low Arctic tundra (Fig. 1). A forest plot (circular area with a 30 m diameter) was established at each site. There, we inventoried tree species, recorded metrics (height, diameter at breast height, crown diameter) and individual trees' GPS coordinates and sampled tree cores (Kruse et al., 2025a, 2025b, 2025c). UAV-based data was acquired for the forest plots (Kruse et al., 2025c, 2025d, 2025f), covering a minimum of a 500 m x 50 m transect using a YellowScan Mapper+ LiDAR sensor with a high-resolution Red Green Blue (RGB) camera (Appendix S1). The forest plot was set in the center of the UAV path and located using the GPS points. Survey paths were flown at a speed of 5 m/s along parallel lines spaced 20 m apart with a 75% overlap at an altitude of 70 m above ground. With this configuration, the LiDAR data have a ground resolution of a minimum of 400 points/  $\mathrm{m}^2$ .

### **Data processing and analyses**

### From UAV-LiDAR point cloud data to forest patches

Figure 2 summarizes the study's workflow, from acquiring UAV data to identifying successional stages of forest patches.

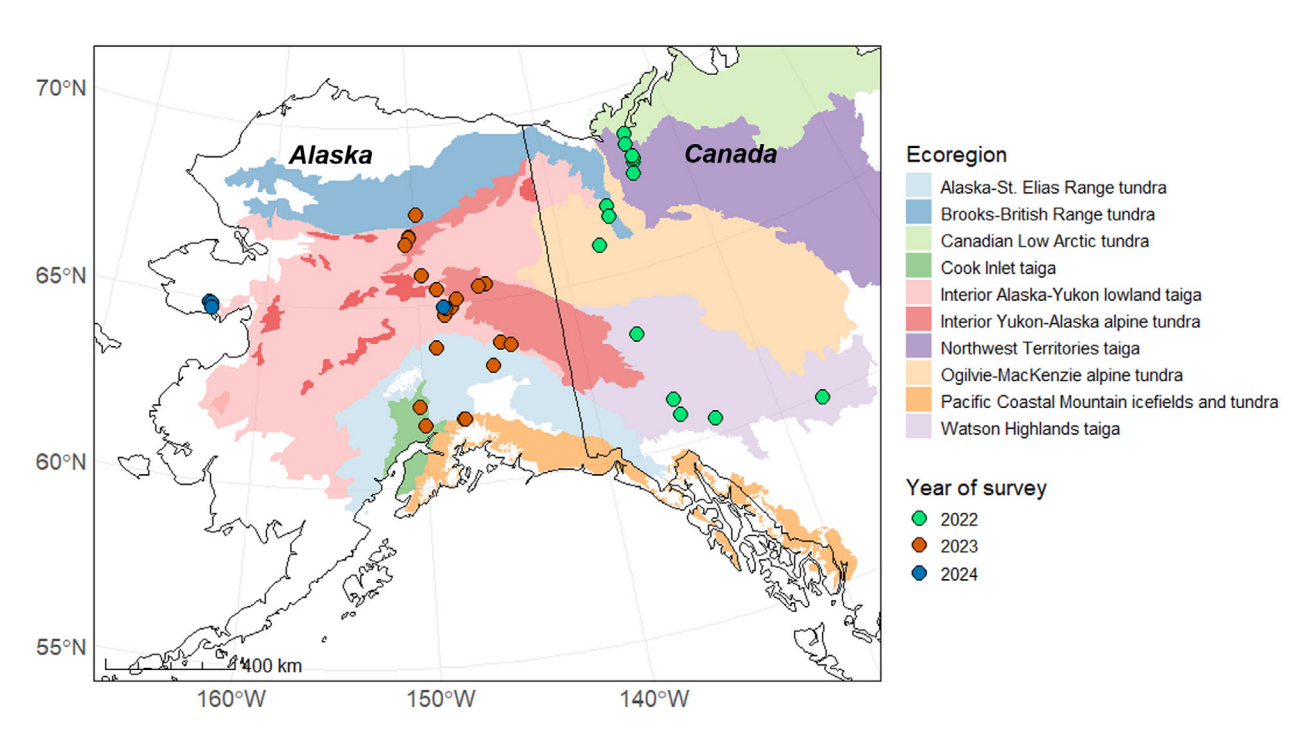


**Figure 1.** Sites of UAV-based acquisitions (N = 48) and forest plots established in the boreal forest during the summers of 2022 in Canada and 2023 and 2024 in Alaska. Different colors represent different expeditions (green, 2022 in Canada; red, 2023 in Alaska; blue, 2024 in Alaska), and the background represents the ecoregions present at sites from the RESOLVE Ecoregions and Biomes dataset (Dinerstein et al., 2017).

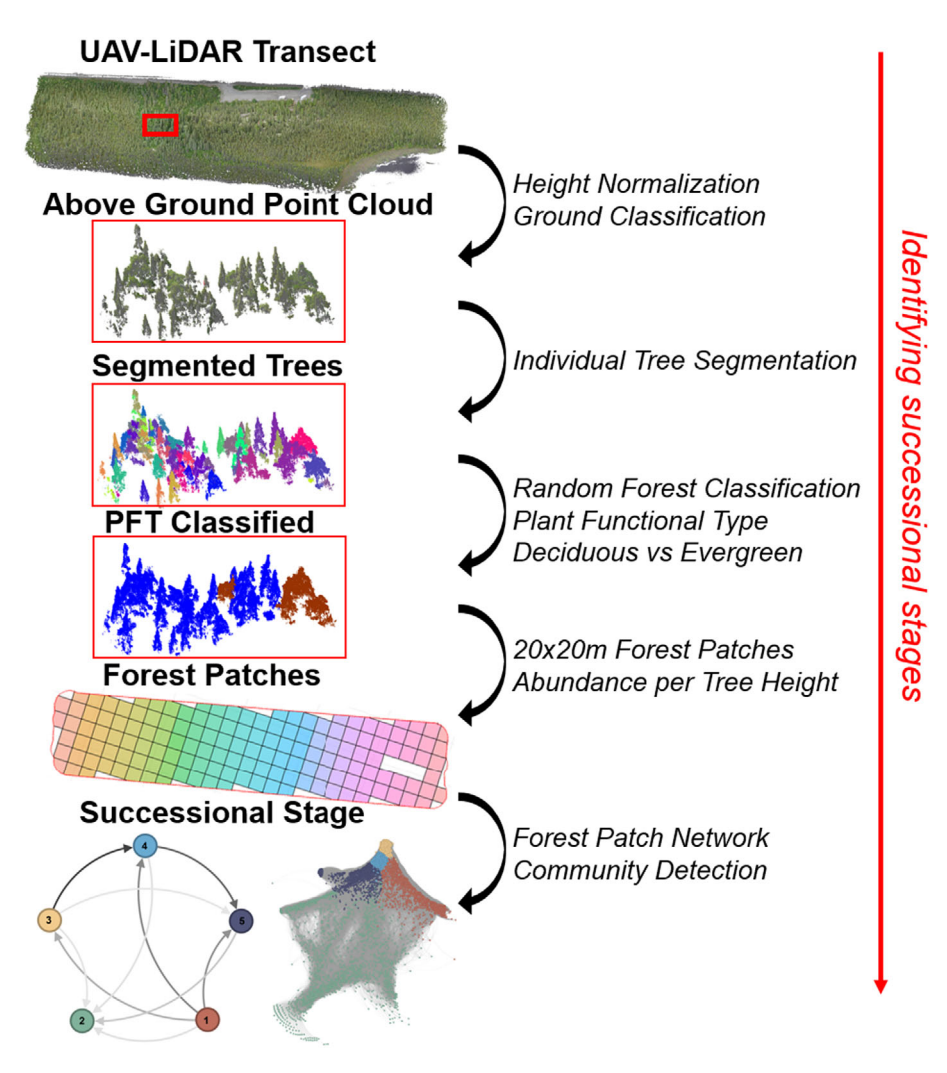


**Figure 2.** Workflow of the study: from UAV-LiDAR point clouds to forest successional stages. The black arrows represent the next step in the workflow. We start by collecting UAV-LiDAR and go through every single step visually described here. This figure shows one example site, with the red box zooming into an area of the site.

### Preprocessing point clouds and individual tree segmentation

We applied a series of processing steps to ensure high-quality point cloud data for analysis. For accurate georeferencing of the point cloud, we first postprocessed the base station location of an EMLID Reach RS2+ Global Navigation Satellite Systems (GNSS) receiver, to further use the observations together with the UAV's GNSS and Inertial Measurement Unit (IMU) observations for precise point positioning (Zumberge et al., 1997) in POSPac UAV software v8.8 (Trimble, Australia). The EMLID Reach was always placed no more than 500 m from the flight locations. Likewise, we georeferenced the RGB images using YellowScan CloudStation, allowing the colorization of the point clouds with three bands: Red, Green and Blue.

We generated digital terrain models (DTM) from the LiDAR data by means of triangulation with the lidR package v4.1.1 (Roussel et al., 2020; Roussel & Auty, 2024). The DTMs were used to normalize the point clouds. We cropped the outer edges of the point clouds to remove low-point cloud density. We classified the points into ground and aboveground using a cloth simulation filter (Zhang et al., 2016) and applied a statistical outlier removal in the CloudCompare software v2.13.beta. We used the 3-D graph–based algorithm Treeiso (Xi & Hopkinson, 2022) in Matlab (The MathWorks Inc, 2024) to segment each site's aboveground point clouds into individual trees. Based on an empirical approach, we optimized the individual tree segmentation with the given parameters for each site, with  $\varepsilon_{\rm max}$ ,  $\varepsilon_{\rm max}$  and proving

**Table 1.** Values of *Treelso* parameters used to segment individual trees.

K <sub>1</sub>	$\lambda_1$	K <sub>2</sub>	$\lambda_2$	Decimated resolution 1 and 2 (m)	$\epsilon_{\text{max}} \ (\text{m})$	$ ho_{\text{max}}$	ω
3	20	10	10	0.05 and 0.1	1.0	2	1
3	20	10	10	0.05 and 0.1	3.0	0.5	0.5

 $K_1$ ,  $K_2$ : Number of nearest neighbors, controlling the unit size of a cluster;  $\lambda_1$ ,  $\lambda_2$ : A regularizing parameter, a greater number producing more edge cuts;  $\epsilon_{max}$ : Maximally allowed threshold distance to consider an edge;  $\rho_{max}$ : Ratio of elevation difference from neighbors to segment length;  $\omega$ : Importance of the horizontal overlapping ratio over the vertical.

particularly effective in differentiating sparsely from densely forested sites. We achieved the best segmentation results with one or the other set of parameters (Table 1).

### Tree structural and spectral metrics

Once individual trees were segmented from the above-ground point cloud data, we derived their structural and spectral attributes (Table 2). Tree height and crown area were computed with the *crown\_metrics* function of the *lidR* package (Roussel et al., 2020; Roussel & Auty, 2024) using R v4.3.2 (R Core Team, 2023) and normalized crown point density (i.e. the number of points in a tree/crown area) with a custom function. Tree height is estimated as the maximum height (Z) value among all LiDAR returns within each crown segment. Crown area is computed by applying a 2D convex hull to the XY coordinates of all points in each crown segment. The convex hull is the smallest convex polygon enclosing all points in the horizontal plane.

Two spectral indices were derived from the colorized point clouds' RGB data: Normalized Green-Red Difference Index (NGRDI) (Tucker, 1979) and the Visible Atmospherically Resistant Index (VARI) (Gitelson et al., 2002). NGRDI and VARI have been found in previous studies to enhance the vegetation signal using visible wavelengths (Ercole et al., 2024; Komarkova et al., 2020; Luo et al., 2022). VARI and NGRDI (Table 2) enhance the visibility of vegetation while minimizing the influence of illumination effects by normalization. Finally, we applied an empirical filter (tree height/crown

diameter < 0.4) and removed trees smaller than 1 m and crown diameters smaller than 0.5 m. This filtering step removes all eventual remaining shrubs or trees out of interest for this study. Additionally, we estimated the age of each tree present in the point clouds using the tree cores collected during our forest inventories and regression models (Appendix S2).

#### Plant functional types identification

Identifying a forest stand's communities is essential to characterize its successional stage. We distinguished two PFT categories, evergreen and deciduous, based on the communities of tree species found in the forest surveys. This grouping was made to reduce errors associated with uncertain species classification but still captures the dominant ecological strategies and structural contrasts relevant to boreal forest succession (Alexander et al., 2012; Herzschuh, 2020). Evergreen corresponds to the community of trees with evergreen needleleaf species such as white spruce and black spruce and is the dominating PFT in our study region. Deciduous corresponds to broadleaf trees: birch, aspen and poplar. These two categories reflect the secondary successional stages of a boreal forest stand, with a high abundance of deciduous trees being an indicator of early to middle stages of development or disturbance stages and a high abundance of evergreen needleleaf trees as an indicator of late-stage forest (Brassard & Chen, 2006; Chapin et al., 2006).

For each site, we created a training and validation dataset (70/30% ratio) by manually labeling 10–15 trees each

**Table 2.** Structural and spectral variables used for the plant functional type classification.

Variable name	Formula	Unit	Туре	Derived from
Tree height	Max (tree height)	m	Structural	LiDAR data
Crown area	Convex hull area: crown_metrics lidR package	m <sup>3</sup>	Structural	LiDAR data
Normalized crown point density	Number of points in a tree Crown Area	Unitless	Structural	LiDAR data
Red (R)	Median per tree	Unitless	Spectral	RGB Camera
Green (G)	Median per tree	Unitless	Spectral	RGB Camera
Blue (B)	Median per tree	Unitless	Spectral	RGB Camera
NGRDI	$NGRDI = \frac{Green - Red}{Green + Red}$	Unitless	Spectral	RGB Camera
VARI	$VARI = \frac{Green - Red}{Green + Red - Blue}$	Unitless	Spectral	RGB Camera

as evergreen or deciduous, in total 20-30 trees per UAV transect, proportional to the number of trees detected per transect. We used geolocalized trees from the forest inventory and the RGB colorized point clouds to facilitate the PFT identification. We trained a random forest classifier (Breiman, 2001) for each site to identify each tree as evergreen or deciduous using the R package randomForest v4.7.1.1 (Liaw & Wiener, 2002). We tuned the classifiers by adjusting the number of trees (ntrees = 100) while all other hyperparameters were kept at their default values. The variables used as input to the classifier were tree height, normalized crown point density, crown area, the individual tree median value of the red, green and blue bands and spectral indexes NGRDI and VARI. The variety of metrics allows the capture of PFT traits based on structural and spectral characteristics. Accuracies were computed based on the validation datasets, and a variable importance analysis was performed using the latter package's importance() function.

### Aggregation to forest patches

For each of the 48 sites, we split the processed LiDAR transects into 20 m x 20 m forest patches, an area large enough to balance spatial resolution and ecological heterogeneity. We computed the abundance of *evergreen* and *deciduous* trees at each forest patch for three height categories representative of successional stages based on our field observations and other studies (Gutsell & Johnson, 2002): below 5 m (early stage), between 5 and 12 m and above 12 m (mature trees). The abundance corresponds to the ratio between the number of trees in one category and the total number of trees for one specific patch. To provide additional ecological context in the network analysis, we estimated the age of each forest patch by deriving the maximum and mean tree age per category per patch.

### **Network analysis**

We used a directed network to identify successional stages present among all forest patches. The network analysis groups patches of similar characteristics together and highlights their interactions with a direction.

### Network construction

We built a directed network with the forest patches (hereafter called forest-patch network) to extract communities and identify their interactions. Directed networks represent interactions between nodes with a source and target direction, modeling the development from one node to another (Leicht & Newman, 2008). Communities are

connected groups of nodes with high probabilities of sharing similarities (Fortunato & Hric, 2016). Here, we defined each forest patch as the network's nodes with abundance variables as the node attributes. We refer to successional stages as communities, where each identified successional stage corresponds to a group of interconnected forest patches.

The six abundance variables (evergreen and deciduous in three height categories) were selected to calculate a Euclidean distance matrix using the R package igraph (Csárdi et al., 2025; Csardi & Nepusz, 2006), measuring the similarity between all nodes (forest patches). A similarity threshold, set at the 15<sup>th</sup> percentile of the distance distribution, was applied to generate an adjacency matrix. This empirically chosen threshold prioritizes connectivity with similar nodes while keeping the network sparse enough to avoid excessive connections (Fornito et al., 2010). Directed edges were established so that edges flowed from source nodes with lower age values to targets with higher evergreen age values. The network was assigned weights to the edges based on the similarity scores. Figure 3 describes the network construction process.

### Network community detection

We extracted the network's community structure and modularity (Girvan & Newman, 2002; Newman, 2006) using the Louvain modularity optimization algorithm (Blondel et al., 2008), allowing identification of large communities. A 'giant component' filter (i.e. Core of the network) was applied to the network, removing isolated nodes and reducing noise. The network's analysis and visualization were performed with Gephi v0.10.1. Based on the community of a node, the corresponding forest patches were manually assigned a successional stage related to the abundance of evergreen and deciduous trees and tree height, supported by our field knowledge and successional theories. The existence of a disturbed stage was supported by the United States Department of Agriculture (USDA) disturbance dataset (Appendix S3).

To identify dominant inter-community interactions, we aggregated the network at the community level into a 'super-network' (Stanley et al., 2018) by grouping nodes and summing all edges, directions and weights between communities.

### Network analyses

The betweenness centrality (BC) measures a node's significance within a network, determining the extent to which it lies on the shortest paths between other pairs of nodes (Freeman, 1977). It reflects the node's role as a bridge or

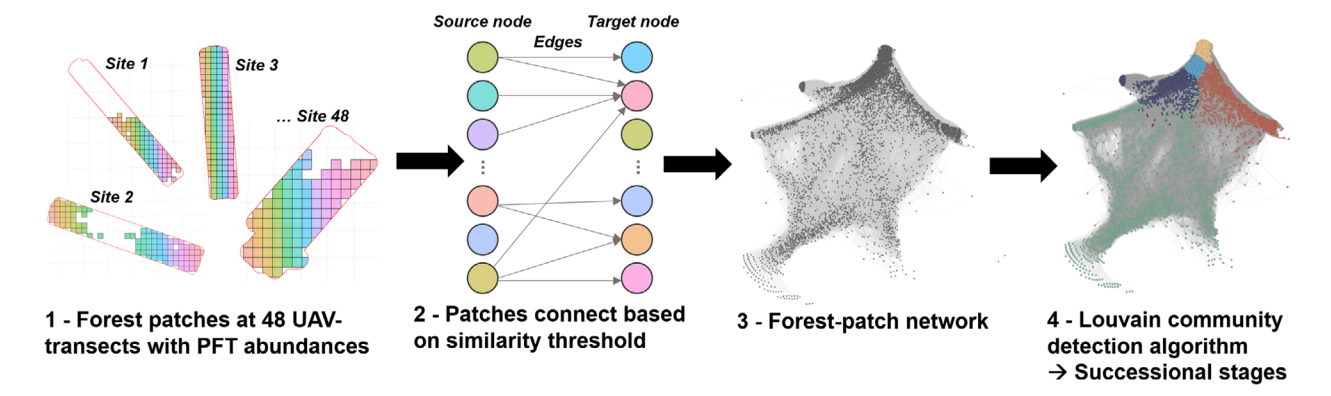


Figure 3. Schematic of the network construction process.

intermediary in facilitating interaction across the network. BC was computed for each node and averaged for each UAV transect, containing multiple forest patches.

#### Forward modeling approach

We modeled the forest patches' trajectories in the future using a simple growth function. This approach gives us a first idea of the trajectories, simplifying the true processes considered in more sophisticated, complex models like LAVESI (Kruse et al., 2016, 2018). Specifically, using tree growth rates derived from the tree height-age regression, we predicted new tree heights and the corresponding forest patches' successional stage membership at a decadal step for the next 120 years with a simple forward growth model. The prediction is based on the existing tree's age at breast height; no recruitment or death is taken into account.

### Results

## Characteristics and classification of plant functional types

The dataset analyses reveal distinct structural characteristics for the *evergreen* and *deciduous* classes (Fig. 4), with *deciduous* trees and *evergreen* trees having higher median heights of 11 and 7 m, respectively. Random Forest (RF) classification accuracies vary across sites, yielding a median overall accuracy of 0.73 with a standard deviation of 0.18 based on the validation datasets. Higher accuracies are observed in homogeneous *evergreen* sites, whereas lower accuracies are more frequently found in mixed forest stands.

Feature importance analyses of the RF classifiers for all sites show that tree height is the most significant variable in differentiating *evergreen* from *deciduous* classes (Fig. 5).

The LiDAR normalized crown point density, the crown area, the NGRDI and VARI, and the RGB camera bands demonstrate a similar level of importance. The spectral variables exhibit the most difference between the class-specific scores. Notably, they play a greater role in predicting *evergreen* over *deciduous* classes.

### Successional stages as inferred by network community detection

### Forest-patch network characteristics

The resulting forest-patch network comprises over three million (3,907,929) directed edges connecting 7,566 nodes. The community detection revealed eleven communities and a modularity of 0.402. The 'giant component' filter identified five major communities (successional stages) with distinct features (Fig. 6A,B). Each stage presents varying abundances of *evergreen* and *deciduous* trees of different heights following a growth succession.

An early development stage was identified, with a high abundance of trees below 5 m, predominantly deciduous species. The second stage is the most diverse, with a substantial deciduous population greater than 5 m, accompanied by a smaller number of evergreen trees of similar height. Moreover, this stage includes shorter deciduous and evergreen trees and a few notably old evergreen trees. We investigated the Insect and Disease Detection Survey by the Forest Service U.S. Department of Agriculture (USDA), which reports forest damage and mortality due to different disturbances (insects, diseases and wind) yearly since 1997 (USDA, 2023). We find that sites with forest patches in this second stage in Alaska were consistently reported as disturbed by defoliation or mortality in the past decade (Appendix S3). These indications suggest it may represent a disturbance stage.

The third stage is marked by a high abundance of *ever-green* below 5 m, with some reaching 12 m. Similarly, the

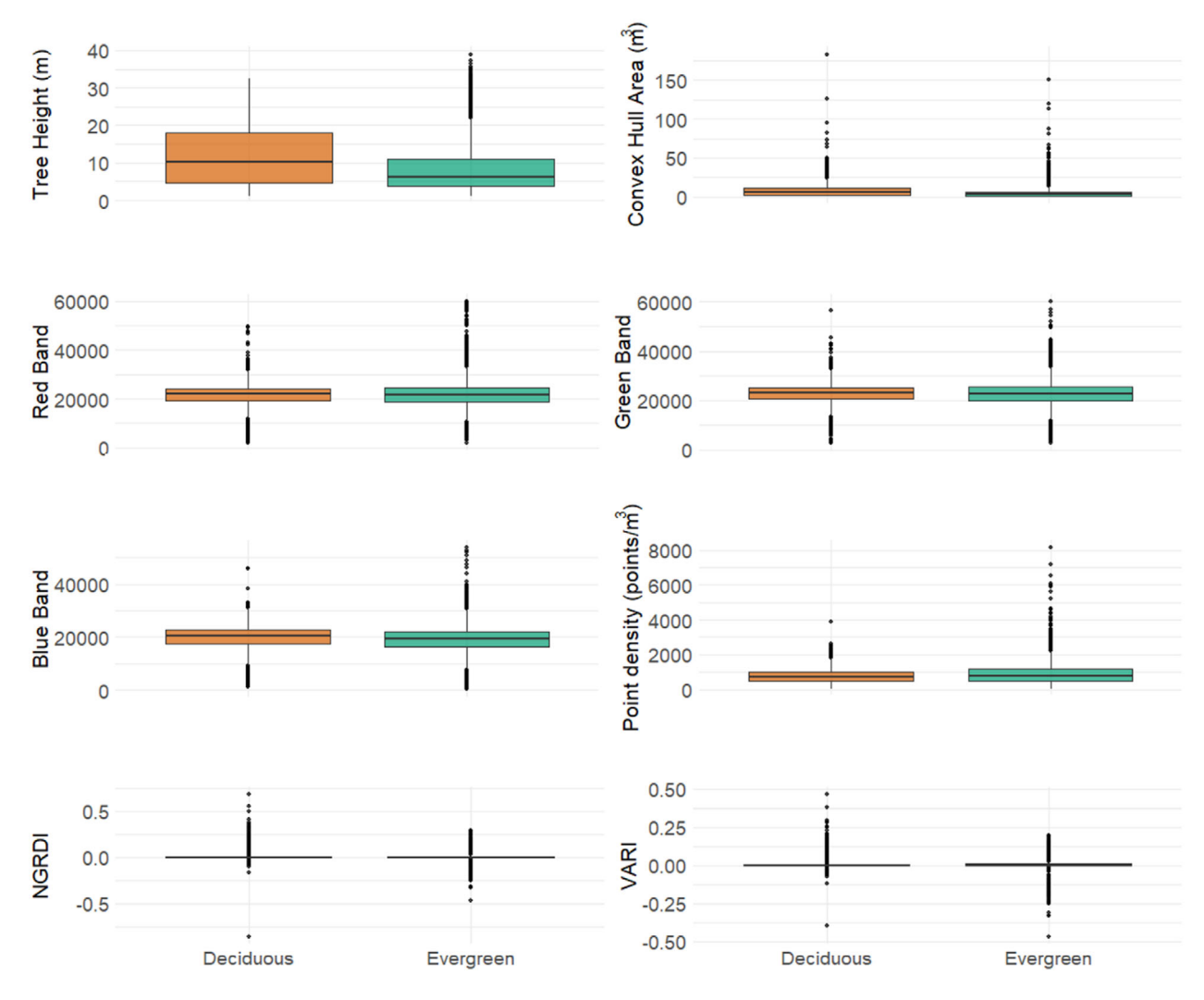


**Figure 4.** Characteristics of the *evergreen* and *deciduous* plant functional types in the datasets used for training the random forest classifiers. RGB values are in 16-bit digital numbers (DN) representing raw sensor readings ranging from 0 (black pixel) to 65,535 (white pixel). *Deciduous* trees have a higher median height than *evergreen* trees.

fourth stage is dominated by evergreen, with more evergreen between 5 and 12 m and slightly less evergreen below 5 m. These two stages (3 and 4) are characteristics of transitional stages, bridging early and late succession with a gradual increase in evergreen abundance and height. The final stage shows the highest abundance of tall evergreen trees, ranging from 5 to 12 m and above, along with a subsequent abundance of smaller evergreen and deciduous trees. This fifth stage represents a late succession stage, such as an old-growth evergreen forest stand.

Each stage contains about the same number of nodes (between 1,306 and 1,898), though some stages are more sparse than others (Fig. 6A). Stages 3 and 4 are clustered at the top of the visualized network, showing distinct features and less similarity with other stages but rather

strong internal connections. Stages 1 and 5 are positioned on opposite sides of the network, demonstrating some clustering but being more dispersed than stages 3 and 4, and therefore sharing more similarities with other stages. Stage 2 is scattered across the network, indicating more heterogeneous patches with less cohesion compared to the other communities. We observe an overlap between stages 1, 2 and 5 at the center of the network, suggesting that similar nodes are shared across these communities. These nodes may serve dual functions as bridges, connecting distant parts of the network with shared similarities.

The super-network allows better identification of interactions between successional stages – here represented as supernodes. Figure 7 shows that all dominant edges originate from the early stage (1), with stronger edges

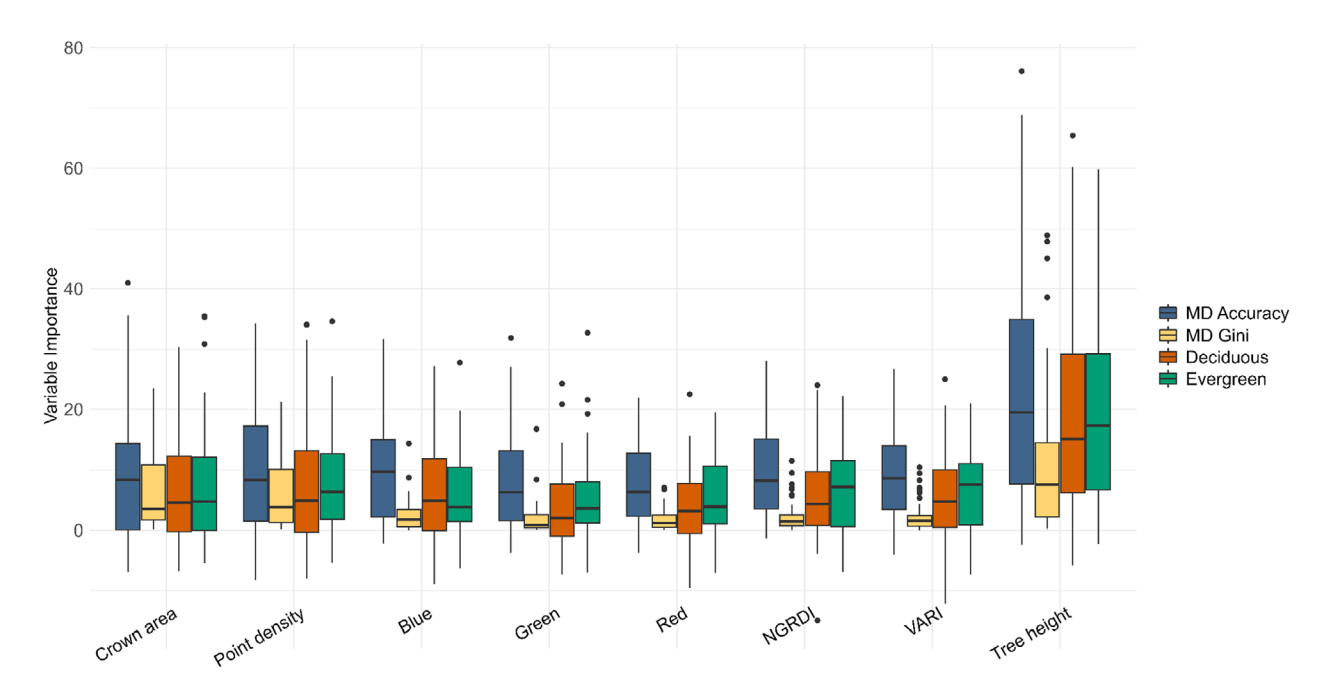


**Figure 5.** Distribution of the variable importance measures for all random forest classifiers. Deciduous (orange) and evergreen (green) are the class-specific importance scores. MD Accuracy is the Mean Decrease Accuracy in the overall model if a given variable is excluded. A high MDA indicates that the variable has an important role in predicting the classes. MD Gini is the Mean Decrease in node impurity when splitting on a given variable. Higher values suggest that the variable plays a significant role in separating the classes.

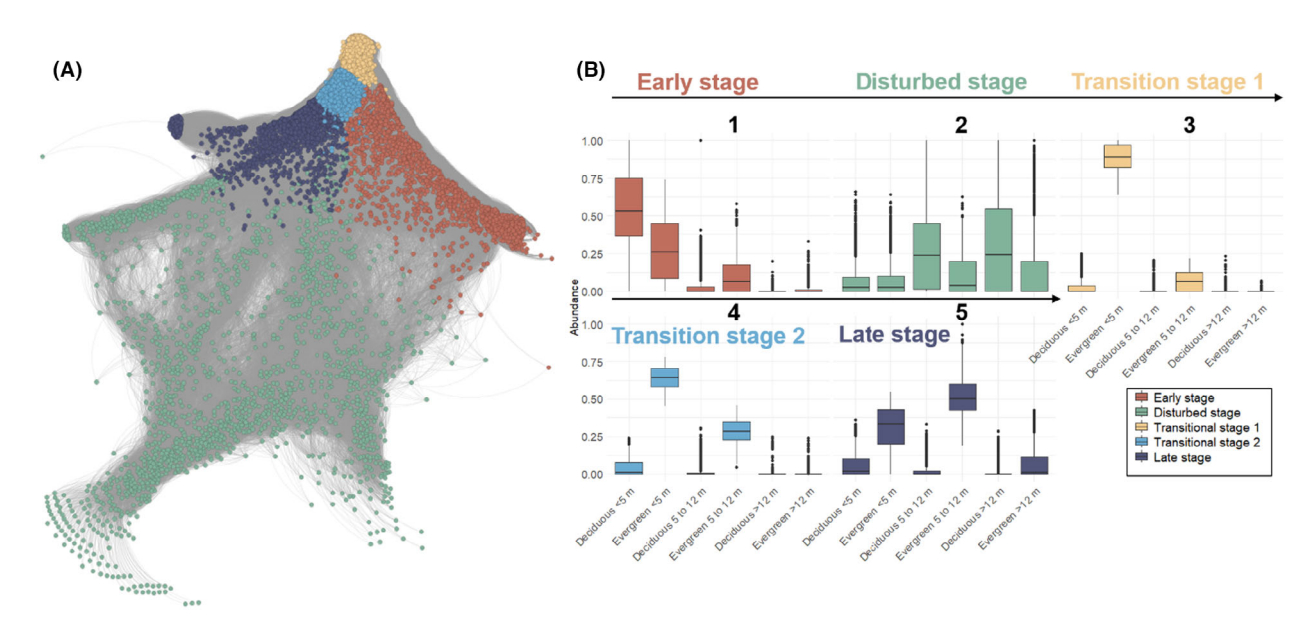


**Figure 6.** (A) Forest-patch network with a Fruchterman-Reingold layout (Fruchterman & Reingold, 1991). Each color represents a unique successional stage, and the edges are gray. (B) Boxplot of the abundance of evergreen and deciduous for three height categories for each detected stage. The black arrow above increasing numbers in panel (B) shows the general succession direction, indicating turns into the next stage, except for the disturbed stage, which is an intermediate stage.

converging into the late stage (5), either passing through the transition stages (3–4) or bypassing them. Stage 2 appears to function predominantly as a sink but has weaker connections with other stages, suggesting that it is more likely to be bypassed than the other stages. The edge percentages connecting supernodes signify that while the

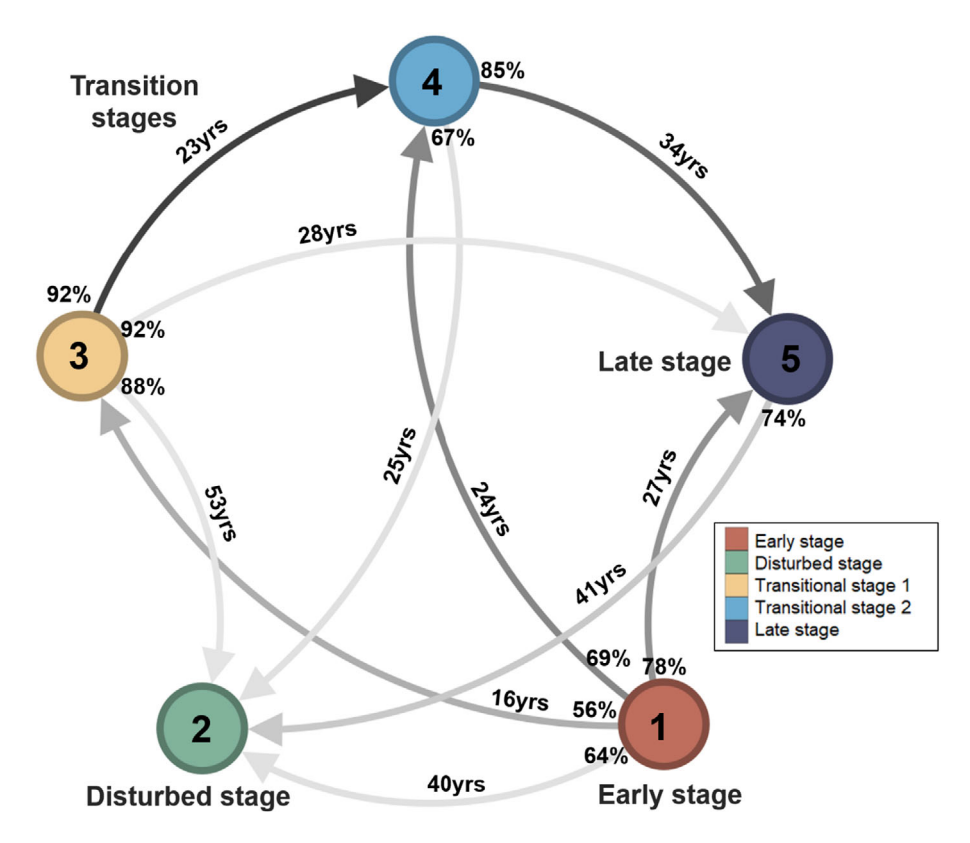


**Figure 7.** Super-network derived from the forest-patch network. Each supernode represents a successional stage, as indicated in the legend. The arrows show the dominant direction of edges between two supernodes, with the percentage of edges between two supernodes going in the dominant direction. The darker the edges, the stronger the connection. The year associated with each edge (e.g. 40 yrs. between stages 1 and 2) shows the age difference between the mean of the oldest tree's age per patch of both stages.

edges show the dominant direction, movement of nodes in the opposite trajectory also occurs.

**Network connectivity** 

To understand the network's connectivity across sites, we analyzed the BC of each node. We selected sites with the lowest, median and highest mean BC and visualized them in the network (Fig. 8A). The density plot shows that the majority of sites are within a normal distribution pattern with comparable BC values close to the median, except for a few sites with higher BC (Fig. 8B). Site EN22055, (a mixed spruce and poplar forest with tall individuals partly disturbed by a recent forest fire in 2021) in Northwest Canada has the highest BC and is located at the center of the network within the disturbed and late stages. This indicates that these nodes (Fig. 8B, red) play a key role in maintaining overall network connectivity. The site with the minimum BC (Fig. 8A, purple) is located at one network's edge, seemingly at terminal positions, and consequently has fewer connections. The median (Fig. 8A, green) serves as a benchmark for comparison, where nodes tend to be more spread out across the network.

### Mapped successional stages

By characterizing forest patches with a successional stage, we can effectively map the forest conditions across our study sites. Early stages are predominantly found in the treeline regions, such as Northwest Canada and western Alaska (respectively northern and western tundra-taiga transition) (Fig. 9). Transitional stages (3 and 4) are primarily located in the northern to central parts of the study area, while late stage's sites are concentrated in the southern part of our study region in Canada. Disturbed sites (stage 2) are more widely distributed across Alaska and Northwest Canada, with a notable cluster in interior and southern Alaska.

### Potential successional stage transition

Using a forward growth model to predict the transition of forest patches to different successional stages provides

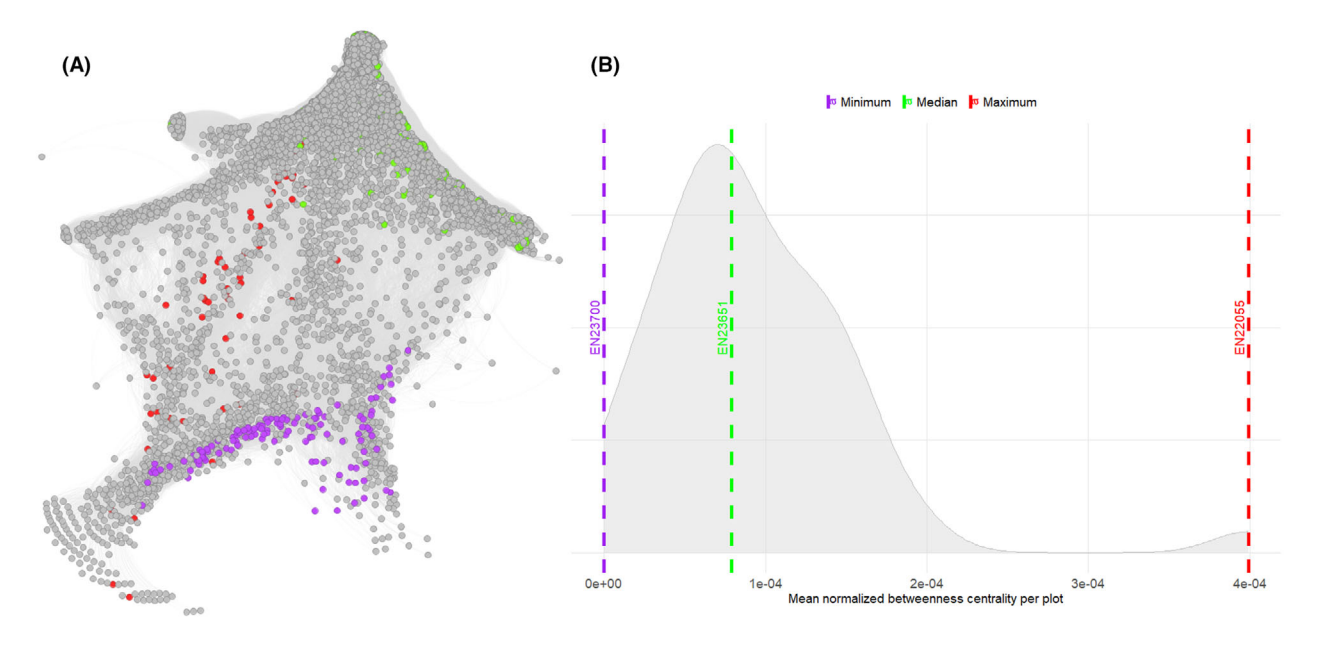


**Figure 8.** Betweenness centrality (BC) across sites. (A) Forest-patch network with nodes highlighted according to the sites' BC: purple is the site with the lowest BC, green is the median BC, and red is the highest BC. (B) Density plot (number of nodes) of mean normalized BC per site. The dashed lines represent the minimum, median and maximum BC.

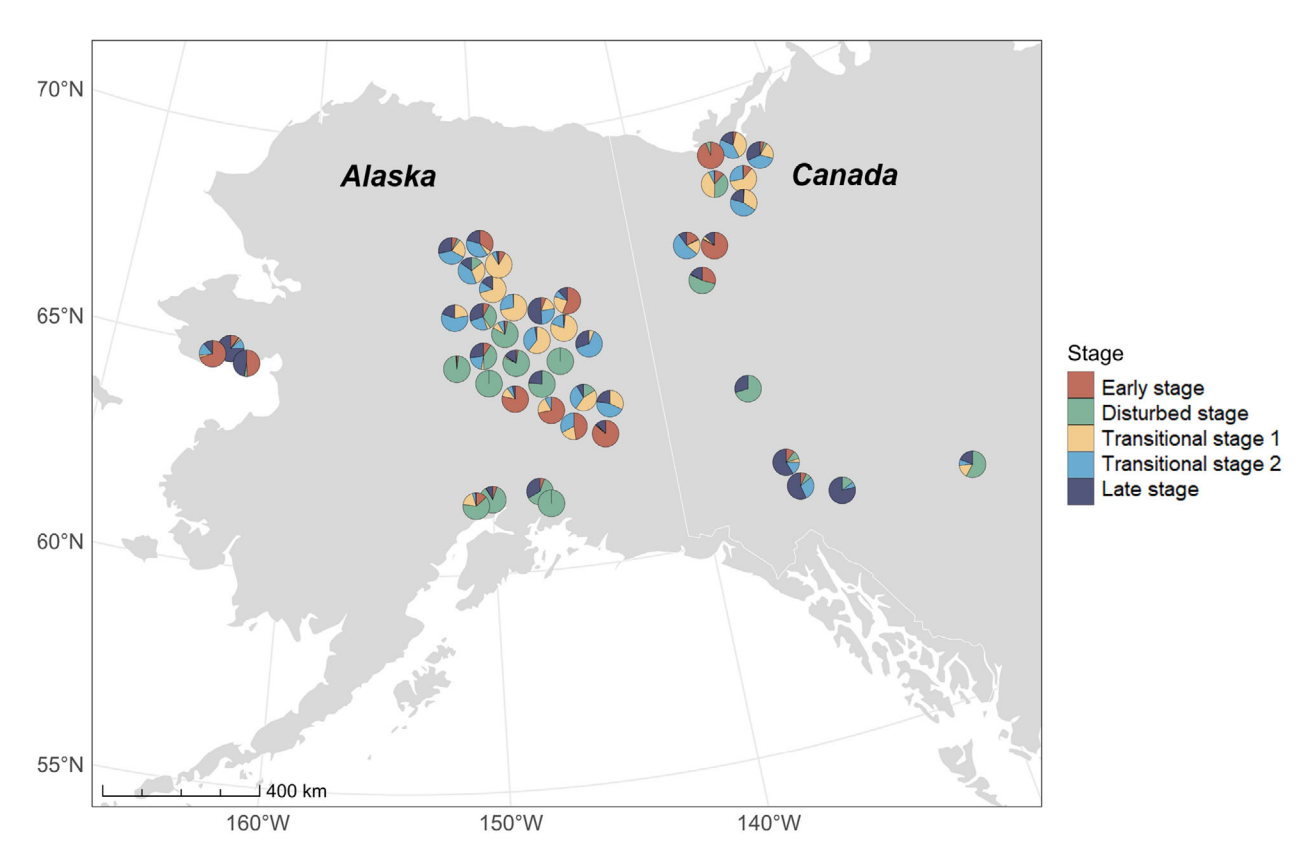


**Figure 9.** Distribution of the successional stages at each site represented as pie charts. Some of them, especially in interior Alaska, are slightly moved to avoid overlap with other close sites; see Fig. 1 and Appendix S4 for their original locations and detailed distribution.

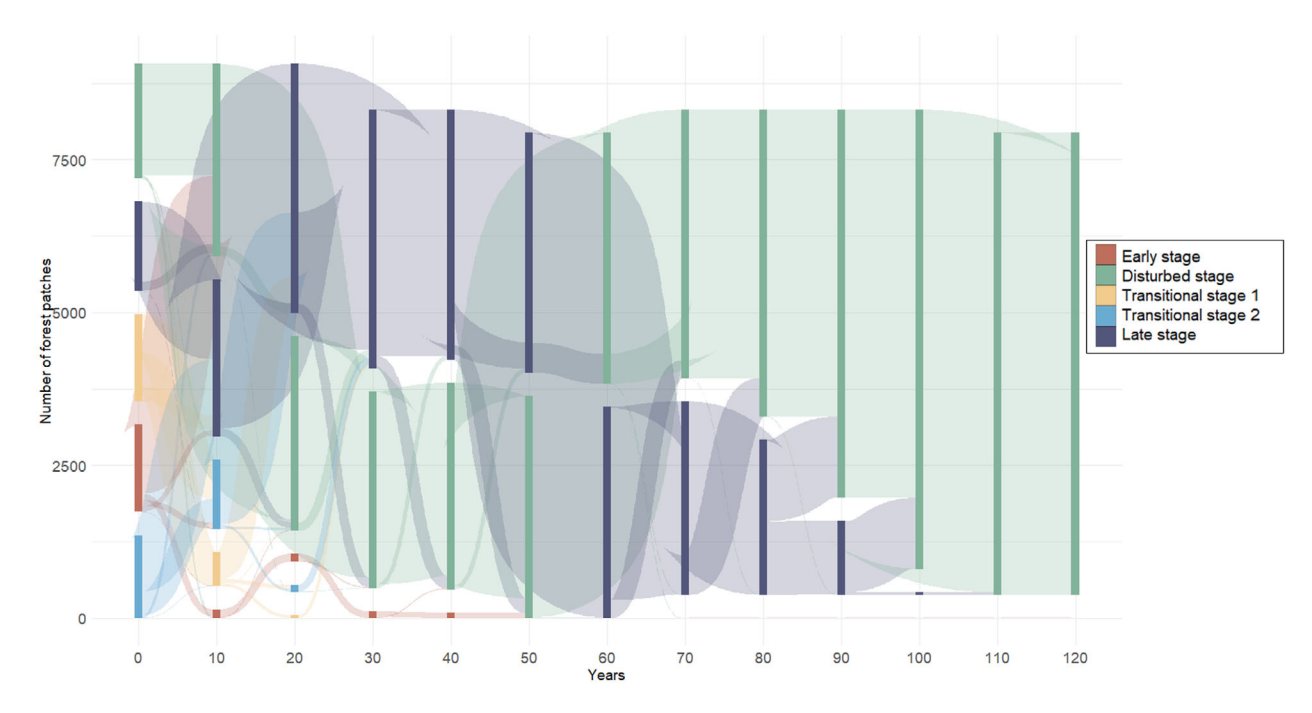


**Figure 10.** Sankey diagram representing the evolution of forest patches' successional stage with a 10-year increment. The y-axis is the number of forest patches in the successional stage, and the x-axis is the years elapsed.

valuable insights into the trajectories of these sites. The Sankey flow diagram visualizes these trajectories over time (Fig. 10). Stages 1, 3 and 4 decrease rapidly after 10 years and shift into the late and disturbed stages (5 and 2). Stages 2 and 5 gradually increase until being co-dominant at 30 years. After that, stage 5 declines, allowing stage 2 to dominate all patches.

### **Discussion**

Leveraging UAV-LiDAR coupled with RGB data and network analyses, we identified successional stages in boreal forests across sites in Alaska and Northwest Canada, providing insights into their trajectories and interactions. Our findings reveal the presence of five interconnected successional stages, each characterized by varying abundances of evergreen and deciduous plant functional types (PFT). Notably, the most diverse stage - corresponding to a disturbed state - is predominantly found in central and south Alaska, whereas old-growth evergreen stands are more common in our southern sites in Canada. By analyzing the development of forest patches, we observed that they all ultimately lead to a disturbed stage within approximately 100 years. These results support our initial hypothesis that UAV-LiDARderived metrics are effective for the classification of PFTs and that network analysis can identify distinct forest successional stages.

### Plant functional type classification based on UAV structural and spectral data

We used high-resolution UAV-derived structural and spectral metrics to classify individual trees into the two plant functional types building random forest classifiers. Consistent with previous studies (Cho et al., 2012; Naidoo et al., 2012) and supporting our initial hypothesis, our findings highlight LiDAR-derived tree height as a key predictor variable. Considering the broad spatial extent, variations in bioclimatic gradients and the heterogeneity of the study sites, we suggest that PFT characteristics also reflect site-specific environmental factors rather than general species characteristics. While our approach of coupling LiDAR and RGB data effectively captured PFTs, species-level tree classification would further refine the definition of successional stages, particularly by differentiating black spruce from white spruce, which indicates different site productivity (Fastie & Ott, 2006). However, achieving this would require a more detailed and species-balanced training and validation dataset, which was not available for this study - despite the considerable dataset size, due to the logistical challenges of data acquisition. Research shows that coupling multispectral or hyperspectral data with LiDAR-derived variables might allow better tree species classification (Dalponte et al., 2008; Ghosh et al., 2014; Zhong et al., 2022), at least for mixed temperate forests. Extended boreal forest

species-level reference datasets from LiDAR point cloud and spectral data are needed for such applications and are currently under development by our research team.

# Successional stages as inferred from community detection in a forest-patch network

Using a community detection in the forest-patch network, we identified five successional stages from early to late development, characterized by varying abundances of evergreen and deciduous PFTs. These findings correspond to observations of species communities and forest succession in the boreal forests (Fastie & Ott, 2006; Viereck et al., 1986). While our analysis establishes these stages, it does not imply that only five discrete stages exist but rather a continuum of interconnected stages, where forest patches dynamically transition in response to environmental conditions and disturbances. We built the network using similarity alone, without restricting connections by geographic distance. To assess potential spatial autocorrelation, we tested additional networks where nodes were only connected if they exceeded distance thresholds of 40 m, 160 m, 300 m or 1,000 m. These constraints slightly modified the network's modularity but did not affect community detection, indicating spatial dependence had a negligible impact on network structure. Unlike traditional clustering methods classifying forest patches solely based on similarity, network-based approaches offer additional insights by revealing the structural connectivity and interactions between patches using edges (Bloomfield et al., 2018), highlighting the dynamic nature of succession. We applied a high similarity threshold to construct a very connected network and employed a community detection method favoring larger communities. This reasoning stems from our objective of identifying broad successional stages rather than smaller communities. Additionally, the network approach enables the identification of key nodes, such as sites with high betweenness centrality serving as critical areas linking multiple successional stages. The strong interactions between the early, transitional and late stages suggest that this trajectory is a dominant one, consistent with established succession theories and observations referring to deciduous stands as early and evergreen stands as late stages (Anyomi et al., 2022; Fastie & Ott, 2006). However, stage 2 (disturbed) stands apart with weaker connections converging from the other stages. This pattern suggests that stage 2 represents an intermediate stage where a subset of forest patches accumulate, corresponding to disturbance events altering forest structure and composition. These findings support our hypothesis that network analysis can effectively identify forest successional stages.

## An intermediate disturbed successional stage

The second stage identified in our study comprises old, young and mixed forests, suggesting it represents a phase of disturbance recovery. In the western North American boreal forest, disturbances such as stand-replacing fires occur regularly, at intervals ranging from 50 to 150 years (Larsen, 1997; Payette, 1992), playing a key role in shaping successional trajectories (Johnstone et al., 2011). Our finding is further supported by the high frequency of disturbed sites overlapping with mapped disturbance areas identified by the USDA (2023) and our field observations on site. In this stage, forest stands are regenerating following structural and compositional changes induced by disturbances such as wildfires or insect outbreaks. In this scenario, some old-growth evergreen trees may persist if they survived the disturbance, while others perished. The subsequent regeneration process favors the establishment of deciduous species in the early stages, explaining the presence of deciduous trees alongside the remaining evergreens (Anyomi et al., 2022).

### Geographical distribution of successional stages

Our study shows the geographical distribution of successional stages across Alaska and western Canada, revealing distinct regional patterns. We identified clusters of disturbed sites in interior and southern Alaska, which are warmer and more fire-influenced regions than other parts of the boreal forests (Beck et al., 2011). Consistent with our findings, Roland et al. (2019) report significantly higher occupancy and abundance of both conifer and broadleaf species in interior Alaska due to disturbances.

We find that the transitional stages are mainly located in northern Canada and Alaska. These regions are characteristic of the biome boundary between boreal forest and tundra, known as the Tundra-Taiga Ecotone (TTE), where trees are shorter and border tundra landscapes (Montesano et al., 2020). Early stages are mainly found on the western Seward Peninsula, a region marked by the longitudinal tundra-taiga boundary (Viereck & Little, 1972). In contrast, our findings indicate that older evergreen stands are primarily located in the southern part of the study region in Canada. A comparison with forest age maps (Besnard et al., 2021) further supports this observation, as this region contains older forests relative to our other study sites.

The spatial patterns in successional stages have important ecological implications. Early and transitional successional stages provide open, resource-rich habitats that support high biodiversity, enhance nutrient cycling and

20563485, 0, Downloaded from https://sslpublications.onlinelibrary.wiley.com/doi/10.1002/rse2.70029 by Helmholtz-Zentrum Potsdam GFZ, Wiley Online Library on [10/11/2025]. See the Terms and Conditions (https://onlinelibrary.wiley.com/terms

and-conditions) on Wiley Online Library for rules of use; OA articles are governed by the applicable Creative Commons Licenso

promote landscape connectivity (Alexander et al., 2012; Anyomi et al., 2022). Old, evergreen-dominated stands create cold, moist understories, leading to permafrost development and reduced nutrient availability. These conditions limit productivity and standing biomass but contribute to long-term soil carbon storage (Alexander et al., 2012; Flanagan & Cleve, 1983; Van Cleve, Oliver, et al., 1983). They also serve as important habitat for fur-bearers and are key sites for berry production (Nelson et al., 2008). In contrast, deciduous-dominated stages (e.g., Disturbed) promote rapid litter decomposition, supporting higher aboveground biomass and productivity (Van Cleve, Dyrness, et al., 1983; Van Cleve, Oliver, et al., 1983). Maintaining a mosaic of successional stages is crucial for sustaining biodiversity and supporting a range of ecosystem functions (Porter et al., 2023).

Since our results are based on subsets of the landscape rather than the entire region, some observed patterns may not fully represent broader trends. While the identified successional stages may reflect a biogeographic or environmental gradient to some extent, our analysis of bioclimatic variables (Fick & Hijmans, 2017) found no evidence of such a gradient in the distribution of successional stages (Appendix S5). Moreover, we acknowledge the uncertainties related to the space for time substitution in our analysis. We captured one-time snapshots of multiple sites for comparison, which may not entirely reflect the true successional change over time that would be observed at a fixed location, where varying trajectories could emerge. However, this approach still provides crucial information about the current patterns found at sites across the boreal forest.

### Implications for future boreal forest succession

The prediction provides insights into the future dynamics of the investigated forest patches, revealing they tend to shift between the late and disturbed stages over 20 years before ultimately reaching a disturbed state after 100 years. This time frame corresponds to the disturbance intervals encountered in the boreal forests, and the approximate time it takes to reach a mature evergreen stand (Fastie & Ott, 2006; Van Cleve & Viereck, 1981). Once a forested area reaches a disturbed state, the disturbance may either be stand-replacing or leave some surviving trees, after which it may gradually move through successional trajectories into different stages. Additionally, with the fire season becoming longer (Flannigan et al., 2013), the interval for vegetation regeneration shortens (Coogan et al., 2019), which in turn leads to more forested areas becoming part of this disturbed stage. However, this prediction is solely based on tree growth estimations, assuming no tree decay, new growth, environmental changes or other disturbances. Considering these factors in a dynamic vegetation model, such as the individual-based and spatially explicit model LAVESI (Kruse et al., 2016, 2018) would allow a more realistic prediction of the dynamics and potentially show a delay of the transition to a disturbed state. While we do not suggest that all boreal forests will become disturbed, our findings reinforce that disturbances significantly shape boreal forest succession in Alaska and Northwestern Canada (Foster et al., 2022).

### **Conclusions**

In this study, we investigated structural and spectral data to assess boreal forest successional stages across sites in Alaska and Northwest Canada. We merged UAV-borne spectral and structural data to classify plant functional types with random forest algorithms, achieving high accuracy in distinguishing coniferous from broadleaf tree species. Based on these results, we built a forest-patch network and detected forest successional stages based on a community detection algorithm.

Our findings revealed five successional stages, ranging from the early stage to the late stage, including a disturbed state. We assessed the geographical distribution of the successional stages, with disturbed sites in interior and southern Alaska and older forests in Canada. Finally, we predicted future dynamics with a forward model and highlighted different successional trajectories.

This study presents a novel application of UAV-LiDAR and RGB data and network analysis, advancing our understanding of successional trajectories across sites in Northwest America up to the northern treeline. Future research could further refine these methods by integrating long-term monitoring and exploring the impacts of climate change on boreal forest succession or upscaling the results with satellite data.

### **Acknowledgments**

We acknowledge the ERC Consolidator Grant Glacial Legacy (772852), BMWi AI-vergreens, DFG-project No. 44865179, and 'Potsdamer InnoLab für Arktisforschung' No. F221-08-AWI/001/002 from the Brandenburg Ministry for Science, Research and Culture (MWFK) for funding this work. We appreciate the support of the DataHub Information Infrastructure funds for support of the Bor-FIT and PC2RCHIVE projects. The authors thank Roy Walluk for field support in the summer of 2024 on the Seward Peninsula, Alaska. Recognizing Indigenous sovereignty, we respectfully acknowledge the Indigenous communities on whose territories we conducted research

20563485, 0, Downloaded from https://zstpublications.onlinelibrary.wiley.com/doi/10.1002/rse2.70029 by Helmholtz-Zentrum Potsdam GFZ, Wiley Online Library on [10/11/2025]. See the Terms and Conditions (https://onlinelibrary.wiley.com/terms

conditions) on Wiley Online Library for rules of use; OA articles are governed by the applicable Creative Commons

across Alaska and Canada, namely, the Inupiat, Gwich'in Nành, Dënéndeh, Koyukon, Tanana, Tanacross, Upper Tanana, Ahtna Nenn', Dena'ina Ełnena, Alutiiq (Sugpiaq), Hän, Lingít Aaní (Tlingit), Kaska Dena Kayeh, Tagish First Nation (Yukon), Tagish, Na-cho Nyak Dun, Selkirk, Tr'ondëk Hwëch'in, Ta'an Kwäch'än, Kwanlin Dün, Denendeh (Acho Dene Koe), Michif Piyii (Métis), Inuvialuit, Inuit Nunangat, Vuntut Gwich'in and Tetlit Gwich'in. We are grateful for the opportunity to work in these territories and recognize the deep cultural, ecological and historical connections Indigenous Peoples have with boreal forests. Open Access funding enabled and organized by Projekt DEAL.

### **Author Contributions**

Léa Enguehard: Conceptualization; investigation; writing — original draft; writing — review and editing; visualization; validation; methodology; software; formal analysis; data curation. Birgit Heim: Conceptualization; funding acquisition. Ulrike Herzschuh: Conceptualization; funding acquisition; project administration. Viktor Dinkel: Methodology. Glenn Juday: Data curation; validation; investigation. Santosh Panda: Data curation. Nicola Falco: Methodology. Jacob Schladebach: Software. Jakob Broers: Software. Stefan Kruse: Conceptualization; investigation; methodology; data curation; supervision; writing — review and editing; resources; project administration.

### **Data Availability Statement**

The code used to generate results is available via: https://github.com/leaenguehard/BorealForest\_Succession\_ LiDAR. The datasets that support this study are published in Pangaea (Enguehard et al., 2025; Felden et al., 2023; Kruse et al., 2025a, 2025b, 2025c, 2025d, 2025e, 2025f).

#### References

- Alexander, H.D., Mack, M.C., Goetz, S., Beck, P.S.A. & Belshe, E.F. (2012) Implications of increased deciduous cover on stand structure and aboveground carbon pools of Alaskan boreal forests. *Ecosphere*, **3**, 1–21. https://doi.org/10.1890/ES11-00364.1
- Almeida, D.R.A., Almeyda Zambrano, A.M., Broadbent, E.N., Wendt, A.L., Foster, P., Wilkinson, B.E. et al. (2020) Detecting successional changes in tropical forest structure using GatorEye drone-borne LiDAR. *Biotropica*, **52**, 1155–1167. https://doi.org/10.1111/btp.12814
- Alonzo, M., Andersen, H.-E., Morton, D. & Cook, B. (2018) Quantifying boreal Forest structure and composition using UAV structure from motion. *Forests*, **9**, 119. https://doi.org/ 10.3390/f9030119

- Anyomi, K.A., Neary, B., Chen, J. & Mayor, S.J. (2022) A critical review of successional dynamics in boreal forests of North America. *Environmental Reviews*, **30**, 563–594. https://doi.org/10.1139/er-2021-0106
- Aquilué, N., Filotas, É., Craven, D., Fortin, M., Brotons, L. & Messier, C. (2020) Evaluating forest resilience to global threats using functional response traits and network properties. *Ecological Applications*, **30**, e02095. https://doi.org/10.1002/eap.2095
- Barbour, M.G. & Christensen, N.L. (1993) Vegetation. In: *Flora of North America north of Mexico*. New York: Oxford University Press, pp. 97–131.
- Beck, P.S.A., Goetz, S.J., Mack, M.C., Alexander, H.D., Jin, Y., Randerson, J.T. et al. (2011) The impacts and implications of an intensifying fire regime on Alaskan boreal forest composition and albedo. *Global Change Biology*, **17**, 2853–2866.
- Belmonte, A., Sankey, T., Biederman, J.A., Bradford, J., Goetz, S.J., Kolb, T. et al. (2020) UAV-derived estimates of forest structure to inform ponderosa pine forest restoration. *Remote Sensing in Ecology and Conservation*, **6**, 181–197. https://doi.org/10.1002/rse2.137
- Bergen, K.M., Goetz, S.J., Dubayah, R.O., Henebry, G.M., Hunsaker, C.T., Imhoff, M.L. et al. (2009) Remote sensing of vegetation 3-D structure for biodiversity and habitat: review and implications for LiDAR and radar spaceborne missions. *Journal of Geophysical Research: Biogeosciences*, **114** (G2), 2008JG000883. https://doi.org/10.1029/2008JG000883
- Bergeron, Y. & Fenton, N.J. (2012) Boreal forests of eastern Canada revisited: old growth, nonfire disturbances, forest succession, and biodiversity. *Botany*, **90**, 509–523. https://doi.org/10.1139/b2012-034
- Besnard, S., Koirala, S., Santoro, M., Weber, U., Nelson, J., Gütter, J. et al. (2021) Mapping global forest age from forest inventories, biomass and climate data. *Earth System Science Data*, **13**, 4881–4896. https://doi.org/10.5194/essd-13-4881-2021
- Blondel, V.D., Guillaume, J.-L., Lambiotte, R. & Lefebvre, E. (2008) Fast unfolding of communities in large networks. *Journal of Statistical Mechanics: Theory and Experiment*, **2008**, P10008. https://doi.org/10.1088/1742-5468/2008/10/P10008
- Bloomfield, N.J., Knerr, N. & Encinas-Viso, F. (2018) A comparison of network and clustering methods to detect biogeographical regions. *Ecography*, **41**, 1–10. https://doi.org/10.1111/ecog.02596
- Bonan, G.B., Pollard, D. & Thompson, S.L. (1992) Effects of boreal forest vegetation on global climate. *Nature*, **359**, 716–718. https://doi.org/10.1038/359716a0
- Brassard, B.W. & Chen, H.Y.H. (2006) Stand structural dynamics of north American boreal forests. *Critical Reviews in Plant Sciences*, **25**, 115–137. https://doi.org/10.1080/07352680500348857

- Brede, B., Barbier, N., Bartholomeus, H., Bartolo, R., Calders, K., Derroire, G. et al. (2021) UAV-laser scanning based metrics for individual tree volume estimation across forest types. In: Hollaus, M. & Pfeifer, N. (Eds.) *Proceedings of the SilviLaser Conference 2021*. Vienna, Austria: Technische Universität Wien. https://doi.org/10.34726/wim.1861
- Breiman, L. (2001) Random forest. In: *Machine learning*. The Netherlands: Kluwer Academic Publishers, pp. 5–32.
- Chapin, F.S., Oswood, M.W., Van Cleve, K., Viereck, L.A. & Verbyla, D.L. (2006) *Alaska's changing boreal forest*. New York, USA: Oxford University Press. https://doi.org/10.1093/oso/9780195154313.001.0001
- Cho, M.A., Mathieu, R., Asner, G.P., Naidoo, L., Van Aardt, J., Ramoelo, A. et al. (2012) Mapping tree species composition in south African savannas using an integrated airborne spectral and LiDAR system. *Remote Sensing of Environment*, **125**, 214–226. https://doi.org/10.1016/j.rse. 2012.07.010
- Coogan, S.C.P., Robinne, F.-N., Jain, P. & Flannigan, M.D. (2019) Scientists' warning on wildfire — a Canadian perspective. *Canadian Journal of Forest Research*, 49, 1015– 1023. https://doi.org/10.1139/cjfr-2019-0094
- Csardi, G. & Nepusz, T. (2006) The igraph software package for complex network research. *InterJournal Complex Systems*, 1695.
- Csárdi, G., Nepusz, T., Müller, K., Horvát, S., Traag, V., Zanini, F. et al. (2025) *igraph for R: R interface of the igraph library for graph theory and network analysis (v2.1.4)*. Zenodo. https://doi.org/10.5281/zenodo.7682609
- Dalponte, M., Bruzzone, L. & Gianelle, D. (2008) Fusion of hyperspectral and LIDAR remote sensing data for classification of complex Forest areas. *IEEE Transactions on Geoscience and Remote Sensing*, 46, 1416–1427. https://doi. org/10.1109/TGRS.2008.916480
- Dinerstein, E., Olson, D., Joshi, A., Vynne, C., Burgess, N.D., Wikramanayake, E. et al. (2017) An ecoregion-based approach to protecting half the terrestrial realm. *Bioscience*, **67**, 534–545. https://doi.org/10.1093/biosci/bix014
- Ercole, T.M., Gomes, J.B.V., Dos Santos Rodrigues, V., Dos Santos Trentin, N., De Oliveira Junior, J.C., Assis-Pereira, G. et al. (2024) VARI as an indicator of site productivity of *Pinus taeda* L.: soil, litter, and plant nutrition. *European Journal of Forest Research*, **143**, 1541–1562. https://doi.org/10.1007/s10342-024-01711-y
- Enguehard, L., Heim, B., Falco, N., Juday, G., Santosh, P., Herzschuh, U. et al. (2025) *UAV LiDAR-based classified trees and species abundance in the boreal forests of Alaska and Northwest Canada [dataset]*. PANGAEA. https://doi.org/10.1594/PANGAEA.977817
- Falkowski, M.J., Evans, J.S., Martinuzzi, S., Gessler, P.E. & Hudak, A.T. (2009) Characterizing forest succession with LiDAR data: an evaluation for the inland northwest, USA.

- Remote Sensing of Environment, 113, 946–956. https://doi.org/10.1016/j.rse.2009.01.003
- Fastie, C.L. & Ott, R.A. (2006) Successional processes in the Alaskan boreal forest. In: Chapin, F.S., Oswood, M.W., Van Cleve, K., Viereck, L.A. & Verbyla, D.L. (Eds.) *Alaska's changing boreal forest.* New York, USA: Oxford University Press, pp. 100–120. https://doi.org/10.1093/oso/9780195154313.003.0012
- Felden, J., Möller, L., Schindler, U., Huber, R., Schumacher, S., Koppe, R. et al. (2023) PANGAEA data Publisher for earth & environmental science. *Scientific Data*, **10**, 347. https://doi.org/10.1038/s41597-023-02269-x
- Fick, S. & Hijmans, R. (2017) WorldClim 2: new 1-km spatial resolution climate surfaces for global land areas. *International Journal of Climatology*, 37, 4302–4315. https://doi.org/10.1002/joc.5086
- Flanagan, P.W. & Cleve, K.V. (1983) Nutrient cycling in relation to decomposition and organic-matter quality in taiga ecosystems. *Canadian Journal of Forest Research*, **13**, 795–817. https://doi.org/10.1139/x83-110
- Flannigan, M., Cantin, A.S., De Groot, W.J., Wotton, M., Newbery, A. & Gowman, L.M. (2013) Global wildland fire season severity in the 21st century. *Forest Ecology and Management*, **294**, 54–61. https://doi.org/10.1016/j.foreco. 2012.10.022
- Fornito, A., Zalesky, A. & Bullmore, E.T. (2010) Network scaling effects in graph analytic studies of human resting-state fMRI data. *Frontiers in Systems Neuroscience*, **4**, 1373. https://doi.org/10.3389/fnsys.2010.00022
- Fortunato, S. & Hric, D. (2016) Community detection in networks: a user guide. *Physics Reports*, **659**, 1–44. https://doi.org/10.1016/j.physrep.2016.09.002
- Fortunato, S. & Newman, M.E.J. (2022) 20 years of network community detection. *Nature Physics*, **18**, 848–850. https://doi.org/10.1038/s41567-022-01716-7
- Foster, A.C., Wang, J.A., Frost, G.V., Davidson, S.J., Hoy, E., Turner, K.W. et al. (2022) Disturbances in north American boreal forest and Arctic tundra: impacts, interactions, and responses. *Environmental Research Letters*, **17**, 113001. https://doi.org/10.1088/1748-9326/ac98d7
- Freeman, L.C. (1977) A set of measures of centrality based on Betweenness. *Sociometry*, **40**, 35. https://doi.org/10.2307/ 3033543
- Fruchterman, T.M.J. & Reingold, E.M. (1991) Graph drawing by force-directed placement. *Software: Practice and Experience*, **21**, 1129–1164. https://doi.org/10.1002/spe. 4380211102
- Fuller, M.M., Wagner, A. & Enquist, B.J. (2008) Using network analysis to characterize forest structure. *Natural Resource Modeling*, **21**, 225–247. https://doi.org/10.1111/j. 1939-7445.2008.00004.x
- Gauthier, S., Bernier, P., Kuuluvainen, T., Shvidenko, A.Z. & Schepaschenko, D.G. (2015) Boreal forest health and global

onlinelibrary.wiley.com/doi/10.1002/rse2.70029 by Helmholtz-Zentrum Potsdam GFZ, Wiley Online Library on [10/11/2025]. See the Terms

and Conditions (https://onlinelibrary.wiley.com/t

litions) on Wiley Online Library for rules of use; OA articles are governed by the applicable Creative Common

- change. Science, **349**, 819–822. https://doi.org/10.1126/science.aaa9092
- Ghosh, A., Fassnacht, F.E., Joshi, P.K. & Koch, B. (2014) A framework for mapping tree species combining hyperspectral and LiDAR data: role of selected classifiers and sensor across three spatial scales. *International Journal of Applied Earth Observation and Geoinformation*, **26**, 49–63. https://doi.org/10.1016/j.jag.2013.05.017
- Girvan, M. & Newman, M.E.J. (2002) Community structure in social and biological networks. *Proceedings of the National Academy of Sciences*, **99**, 7821–7826. https://doi.org/10.1073/pnas.122653799
- Gitelson, A.A., Kaufman, Y.J., Stark, R. & Rundquist, D. (2002) Novel algorithms for remote estimation of vegetation fraction. *Remote Sensing of Environment*, **80**, 76–87. https://doi.org/10.1016/S0034-4257(01)00289-9
- Grime, J.P. (1979) Primary strategies in plants. *Transactions of the Botanical Society of Edinburgh*, **43**, 151–160. https://doi.org/10.1080/03746607908685348
- Guimarães, N., Pádua, L., Marques, P., Silva, N., Peres, E. & Sousa, J.J. (2020) Forestry remote sensing from unmanned aerial vehicles: a review focusing on the data, processing and potentialities. *Remote Sensing*, 12(6), 1046. https://doi.org/ 10.3390/rs12061046
- Gutsell, S.L. & Johnson, E.A. (2002) Accurately ageing trees and examining their height-growth rates: implications for interpreting forest dynamics. *Journal of Ecology*, **90**, 153–166. https://doi.org/10.1046/j.0022-0477.2001.00646.x
- Herzschuh, U. (2020) Legacy of the last glacial on the present-day distribution of deciduous versus evergreen boreal forests. *Global Ecology and Biogeography*, **29**, 198–206. https://doi.org/10.1111/geb.13018
- Huston, M. & Smith, T. (1987) Plant succession: life history and competition. *The American Naturalist*, **130**, 168–198. https://doi.org/10.1086/284704
- Johnstone, J.F., Rupp, T.S., Olson, M. & Verbyla, D. (2011) Modeling impacts of fire severity on successional trajectories and future fire behavior in Alaskan boreal forests. *Landscape Ecology*, 26, 487–500. https://doi.org/10.1007/s10980-011-9574-6
- Kayes, I. & Mallik, A. (2020) Boreal forests: distributions, biodiversity, and management. In: Leal Filho, W., Azul, A.M., Brandli, L., Lange Salvia, A. & Wall, T. (Eds.) *Life on land, encyclopedia of the UN sustainable development goals*. Cham: Springer International Publishing, pp. 1–12. https://doi.org/10.1007/978-3-319-71065-5\_17-1
- Komarkova, J., Jech, J. & Sedlak, P. (2020) Comparison of vegetation spectral indices based on UAV data: land cover identification near small water bodies. In: *Presented at the 2020 15th Iberian Conference on Information Systems and Technologies (CISTI)*. Sevilla, Spain: IEEE, pp. 1–4. https://doi.org/10.23919/CISTI49556.2020.9140899
- Kruse, S., Sevke, F., Zens, N., Baake, A. & Enguehard, L. (2025a) Ring width chronologies (N = 91) from the three

- boreal forest tree species and shrub (alder) across a bioclimatic gradient in western Alaska at the lower Seward Peninsula sampled in 2024. PANGAEA. https://doi.org/10.1594/PANGAEA.981202
- Kruse, S., Haupt, S. & Wei, L. (2025b) Ring width chronologies (N = 181) from seven boreal forest tree species and shrubs (willows) across a bioclimatic gradient in Alaska sampled in 2023. PANGAEA. https://doi.org/10.1594/PANGAEA.981212
- Kruse, S., Haupt, S., Hao, K., Franke, J., Muske, D. & Lohse, M. (2025c) Ring width chronologies (N = 243) from nine boreal forest tree species across a long bioclimatic gradient in northwestern Canada sampled in 2022. PANGAEA. https:// doi.org/10.1594/PANGAEA.981201
- Kruse, S., Enguehard, L., Juday, G., Panda, S., Badola, A., Broers, J. et al. (2025d) Point clouds with ground point classification and individual tree segmentation of 28 northern boreal forest and tundra sites from UAV-based lidar surveys in western and central parts of Alaska in 2024. PANGAEA. https://doi.org/10.1594/PANGAEA.980757
- Kruse, S., Enguehard, L., Juday, G., Panda, S., Badola, A., Broers, J. et al. (2025e) Point clouds with ground point classification and individual tree segmentation of 47 northern boreal forest and tundra sites from UAV-based lidar surveys in the eastern part of Alaska in 2023. PANGAEA. https://doi.org/10.1594/PANGAEA.980485
- Kruse, S., Gloy, J., Farkas, L., Schladebach, J., Hao, K., Döpper, V. et al. (2025f) Point clouds with ground point classification and individual tree segmentation of 25 northern boreal forest and tundra sites from UAV-based lidar surveys in northwestern Canada. PANGAEA. https://doi.org/10.1594/PANGAEA.977771
- Kruse, S., Gerdes, A., Kath, N.J. & Herzschuh, U. (2018)
  Implementing spatially explicit wind-driven seed and pollen dispersal in the individual-based larch simulation model:
  LAVESI-WIND 1.0. Geoscientific Model Development, 11, 4451–4467. https://doi.org/10.5194/gmd-11-4451-2018
- Kruse, S., Wieczorek, M., Jeltsch, F. & Herzschuh, U. (2016)
  Treeline dynamics in Siberia under changing climates as inferred from an individual-based model for Larix. *Ecological Modelling*, 338, 101–121. https://doi.org/10.1016/j.ecolmodel.2016.08.003
- Kuuluvainen, T. (2009) Forest management and biodiversity conservation based on natural ecosystem dynamics in northern Europe: the complexity challenge. *Ambio*, **38**, 309–315. https://doi.org/10.1579/08-A-490.1
- Kuuluvainen, T. & Gauthier, S. (2018) Young and old forest in the boreal: critical stages of ecosystem dynamics and management under global change. *Forest Ecosystems*, 5, 26. https://doi.org/10.1186/s40663-018-0142-2
- Lafleur, B., Fenton, N.J., Simard, M., Leduc, A., Paré, D., Valeria, O. et al. (2018) Ecosystem management in paludified boreal forests: enhancing wood production, biodiversity, and carbon sequestration at the landscape level.

- Forest Ecosystems, 5, 27. https://doi.org/10.1186/s40663-018-0145-z
- Larsen, C.P.S. (1997) Spatial and temporal variations in boreal forest fire frequency in northern Alberta. *Journal of Biogeography*, **24**, 663–673. https://doi.org/10.1111/j.1365-2699.1997.tb00076.x
- Lau, M.K., Borrett, S.R., Baiser, B., Gotelli, N.J. & Ellison, A.M. (2017) Ecological network metrics: opportunities for synthesis. *Ecosphere*, 8, e01900. https://doi.org/10.1002/ecs2. 1900
- Leicht, E.A. & Newman, M.E.J. (2008) Community structure in directed networks. *Physical Review Letters*, **100**, 118703. https://doi.org/10.1103/PhysRevLett.100.118703
- Liaw, A. & Wiener, M. (2002) Classification and regression by random forest. *R News*, 2, 18–22.
- Lu, J., Wang, H., Qin, S., Cao, L., Pu, R., Li, G. et al. (2020) Estimation of aboveground biomass of Robinia pseudoacacia forest in the Yellow River Delta based on UAV and backpack LiDAR point clouds. *International Journal of Applied Earth Observation and Geoinformation*, 86, 102014. https://doi.org/10.1016/j.jag.2019.102014
- Luo, M., Tian, Y., Zhang, S., Huang, L., Wang, H., Liu, Z. et al. (2022) Individual tree detection in coal mine afforestation area based on improved faster RCNN in UAV RGB images. *Remote Sensing*, 14(21), 5545. https://doi.org/10.3390/rs14215545
- Maesano, M., Santopuoli, G., Moresi, F., Matteucci, G., Lasserre, B. & Scarascia Mugnozza, G. (2022) Above ground biomass estimation from UAV high resolution RGB images and LiDAR data in a pine forest in southern Italy. *iForest*, 15, 451–457. https://doi.org/10.3832/ifor3781-015
- Massey, R., Rogers, B.M., Berner, L.T., Cooperdock, S., Mack, M.C., Walker, X.J. et al. (2023) Forest composition change and biophysical climate feedbacks across boreal North America. *Nature Climate Change*, **13**, 1368–1375. https://doi.org/10.1038/s41558-023-01851-w
- Montesano, P.M., Neigh, C.S.R., Macander, M., Feng, M. & Noojipady, P. (2020) The bioclimatic extent and pattern of the cold edge of the boreal forest: the circumpolar taiga-tundra ecotone. *Environmental Research Letters*, **15**, 105019. https://doi.org/10.1088/1748-9326/abb2c7
- Naidoo, L., Cho, M.A., Mathieu, R. & Asner, G. (2012)
  Classification of savanna tree species, in the greater Kruger
  National Park region, by integrating hyperspectral and
  LiDAR data in a random Forest data mining environment.
  ISPRS Journal of Photogrammetry and Remote Sensing, 69,
  167–179. https://doi.org/10.1016/j.isprsjprs.2012.03.005
- Nelson, J.L., Zavaleta, E.S. & Chapin, F.S. (2008) Boreal fire effects on subsistence resources in Alaska and adjacent Canada. *Ecosystems*, **11**, 156–171. https://doi.org/10.1007/s10021-007-9114-z
- Newman, M.E.J. (2006) Modularity and community structure in networks. *Proceedings of the National Academy of Sciences*, 103, 8577–8582. https://doi.org/10.1073/pnas.0601602103

- Pan, Y., Birdsey, R.A., Fang, J., Houghton, R., Kauppi, P.E., Kurz, W.A. et al. (2011) A large and persistent carbon sink in the World's forests. *Science*, **333**, 988–993. https://doi.org/10.1126/science.1201609
- Payette, S. (1992) Fire as a controlling process in the north American boreal forest. In: Shugart, H.H., Leemans, R. & Bonan, G.B. (Eds.) *A systems analysis of the global boreal Forest.* Cambridge: Cambridge University Press, pp. 144–169. https://doi.org/10.1017/CBO9780511565489.006
- Porter, T.M., Smenderovac, E., Morris, D. & Venier, L. (2023) All boreal forest successional stages needed to maintain the full suite of soil biodiversity, community composition, and function following wildfire. *Scientific Reports*, **13**, 7978. https://doi.org/10.1038/s41598-023-30732-7
- R Core Team. (2023) R: a language and environment for statistical computing. Vienna, Austria: R Foundation for Statistical Computing.
- Roland, C.A., Schmidt, J.H., Winder, S.G., Stehn, S.E. & Nicklen, E.F. (2019) Regional variation in interior Alaskan boreal forests is driven by fire disturbance, topography, and climate. *Ecological Monographs*, **89**, e01369. https://doi.org/10.1002/ecm.1369
- Roussel, J.-R. & Auty, D. (2024) Airborne LiDAR data manipulation and visualization for forestry applications. R package version 4.1.1. https://cran.r-project.org/package=lidR
- Roussel, J.-R., Auty, D., Coops, N.C., Tompalski, P., Goodbody, T.R.H., Meador, A.S. et al. (2020) lidR: an R package for analysis of airborne laser scanning (ALS) data. *Remote Sensing of Environment*, **251**, 112061. https://doi.org/10.1016/j.rse.2020.112061
- Scheeres, J., De Jong, J., Brede, B., Brancalion, P.H.S., Broadbent, E.N., Zambrano, A.M.A. et al. (2023)
  Distinguishing forest types in restored tropical landscapes with UAV-borne LiDAR. *Remote Sensing of Environment*, 290, 113533. https://doi.org/10.1016/j.rse.2023.113533
- Shugart, H.H., Saatchi, S. & Hall, F.G. (2010) Importance of structure and its measurement in quantifying function of forest ecosystems. *Journal of Geophysical Research:*Biogeosciences, 115(G2), 2009JG000993. https://doi.org/10.1029/2009JG000993
- Stanley, N., Kwitt, R., Niethammer, M. & Mucha, P.J. (2018) Compressing networks with super nodes. *Scientific Reports*, **8**, 10892. https://doi.org/10.1038/s41598-018-29174-3
- The MathWorks Inc. (2024) *MATLAB version 2024a*. Natick, Massachusetts: The MathWorks Inc. https://www.mathworks.com
- Tucker, C.J. (1979) Red and photographic infrared linear combinations for monitoring vegetation. *Remote Sensing of Environment*, **8**, 127–150. https://doi.org/10.1016/0034-4257 (79)90013-0
- USDA. (2023) USDA forest service forest health protection.

  Insect and Disease Detection Survey (IDS) data downloads.

.onlinelibrary.wiley.com/doi/10.1002/rse2.70029 by Helmholtz

Zentrum Potsdam GFZ, Wiley Online Library on [10/11/2025]. See the Terms

- Ustin, S.L. & Xiao, Q.F. (2001) Mapping successional boreal forests in interior central Alaska. *International Journal of Remote Sensing*, **22**, 1779–1797. https://doi.org/10.1080/01431160118269
- Van Cleve, K., Chapin, F.S., Dyrness, C.T. & Viereck, L.A. (1991) Element cycling in taiga forests: state-factor control. *Bioscience*, 41, 78–88. https://doi.org/10.2307/1311560
- Van Cleve, K., Dyrness, C.T., Viereck, L.A., Fox, J., Chapin, F.S. & Oechel, W. (1983) Taiga ecosystems in interior Alaska. *Bioscience*, 33, 39–44. https://doi.org/10.2307/1309243
- Van Cleve, K., Oliver, L., Schlentner, R., Viereck, L.A. & Dyrness, C.T. (1983) Productivity and nutrient cycling in taiga forest ecosystems. *Canadian Journal of Forest Research*, 13, 747–766. https://doi.org/10.1139/x83-105
- Van Cleve, K. & Viereck, L.A. (1981) Forest succession in relation to nutrient cycling in the boreal Forest of Alaska.
  In: West, D.C., Shugart, H.H. & Botkin, D.B. (Eds.) Forest succession: concepts and application. New York: Springer, pp. 185–211. https://doi.org/10.1007/978-1-4612-5950-3\_13
- Van Ewijk, K.Y., Treitz, P.M. & Scott, N.A. (2011)
  Characterizing Forest succession in Central Ontario using
  LiDAR-derived indices. *Photogrammetric Engineering &*Remote Sensing, 77, 261–269. https://doi.org/10.14358/PERS.
  77.3.261
- Vedrova, E.F., Mukhortova, L.V. & Trefilova, O.V. (2018) Contribution of old growth forests to the carbon budget of the boreal zone in Central Siberia. *Biology Bulletin*, 45, 288– 297. https://doi.org/10.1134/S1062359018030111
- Viereck, L.A. & Little, E.L., Jr. (1972) Alaska trees and shrubs. In: Agriculture Handbook 410. Washington, DC: USDA Forest Service.
- Viereck, L.A., Van Cleve, K. & Dyrness, C.T. (1986) Forest ecosystem distribution in the taiga environment. In: Van Cleve, K., Chapin, F.S., Flanagan, P.W., Viereck, L.A. & Dyrness, C.T. (Eds.) Forest ecosystems in the Alaskan taiga: a synthesis of structure and function. New York: Springer, pp. 22–43. https://doi.org/10.1007/978-1-4612-4902-3\_3
- Watson, J.E.M., Evans, T., Venter, O., Williams, B., Tulloch, A., Stewart, C. et al. (2018) The exceptional value of intact forest ecosystems. *Nature Ecology & Evolution*, **2**, 599–610. https://doi.org/10.1038/s41559-018-0490-x
- Weber, M.G. & Van Cleve, K. (2005) The boreal forests of North America. In: Andersson, F. (Ed.) *Ecosystems of the*

- world. Vol. 6. Coniferous forests. New York, NY: Elsevier Press, pp. 101–130.
- White, J.C., Coops, N.C., Wulder, M.A., Vastaranta, M., Hilker, T. & Tompalski, P. (2016) Remote sensing Technologies for Enhancing Forest Inventories: a review. *Canadian Journal of Remote Sensing*, **42**, 619–641. https://doi.org/10.1080/07038992.2016.1207484
- Worsham, H.M., Wainwright, H.M., Powell, T.L., Falco, N. & Kueppers, L.M. (2025) Abiotic influences on continuous conifer forest structure across a subalpine watershed. *Remote Sensing of Environment*, **318**, 114587. https://doi.org/10.1016/j.rse.2024.114587
- Xi, Z. & Hopkinson, C. (2022) 3D graph-based individual-tree isolation (Treeiso) from terrestrial laser scanning point clouds. *Remote Sensing*, 14(23), 6116. https://doi.org/10. 3390/rs14236116
- Zhang, H., Lin, S., Yu, Q., Gao, G., Xu, C. & Huang, H. (2023) A novel Forest EcoSpatial network for carbon stocking using complex network theory in the Yellow River Basin. *Remote Sensing*, **15**, 2612. https://doi.org/10.3390/rs15102612
- Zhang, W., Qi, J., Wan, P., Wang, H., Xie, D., Wang, X. et al. (2016) An easy-to-use airborne LiDAR data filtering method based on cloth simulation. *Remote Sensing*, **8**, 501. https://doi.org/10.3390/rs8060501
- Zhong, H., Lin, W., Liu, H., Ma, N., Liu, K., Cao, R. et al. (2022) Identification of tree species based on the fusion of UAV hyperspectral image and LiDAR data in a coniferous and broad-leaved mixed forest in Northeast China. *Frontiers in Plant Science*, 13, 964769. https://doi.org/10.3389/fpls. 2022.964769
- Zumberge, J.F., Heflin, M.B., Jefferson, D.C., Watkins, M.M. & Webb, F.H. (1997) Precise point positioning for the efficient and robust analysis of GPS data from large networks. *Journal of Geophysical Research: Solid Earth*, **102**, 5005–5017. https://doi.org/10.1029/96JB03860

### **Supporting Information**

Additional supporting information may be found online in the Supporting Information section at the end of the article.

Appendix S1.